Journal of The Electrochemical Society, **147** (1) 176-188 (2000)
S0013-4651(99)02-063-7 CCC: $7.00

Acid-Based Etching of Silicon Wafers: Mass-Transfer and Kinetic Effects

Milind S. Kulkarni*,z and Henry F. Erk

MEMC Electronic Materials, Incorporated, Saint Peters, Missouri 63376-0008, USA

A study to understand the transport and kinetic effects in three-phase, acid-based wet etching of silicon has been accomplished. Reactants overcome the liquid-phase mass-transfer resistance and the kinetic resistance to complete the reaction. The gaseous bubbles formed by the reaction adhere to random sites on the surface and, thus, mask a fraction of the surface from the reactants. This bubble masking effect is modeled as the bubble transport resistance that acts in parallel with the liquid-phase mass-transfer resistance. These transport effects are lumped into an effective mass-transport resistance, which acts in series with the kinetic resistance. It is shown that the etched surface morphology is a function of the ratio of the effective mass-transport resistance to the kinetic resistance. A rough surface is a field of peaks and valleys. It is theorized that under mass-transfer influence, etch rates at peaks are higher than etch rates at valleys. Hence, the surface is chemically polished. It is shown that the polishing efficiency increases with increasing ratio of mass-transfer resistance to the kinetic resistance, reaches a maximum, and then decreases. Effects of mass-transfer and kinetics on the surface roughness and gloss are explained by both the developed phenomenological model and experimental data.

Manuscript submitted February 16, 1999; revised manuscript received August 9, 1999.

Polished silicon wafers are prepared through various mechanical and chemical processes. First, the silicon single-crystal ingot is sliced into circular disks (wafers) by slicing followed by a flattening process called lapping that involves scrubbing the wafers using an abrasive slurry.[1] The mechanical damage induced during the previous shaping processes is removed by etching which is the focus of this paper. Etching is followed by various unit operations such as polishing and cleaning before it is ready for device fabrication.

Chemical etching of silicon wafers is accomplished by dipping the wafers in an etchant which is traditionally an acidic mixture of HNO_3 + HF and a diluent or a caustic solution of KOH. Various studies in caustic crystallographic etching are reported.[2-4] However, this paper focuses on the transport and kinetic effects only on acid-based etches. Acid etching in HNO_3 + HF mixture is reported to proceed with following global reactions[1]

$$Si + 4HNO_3 \rightarrow SiO_2 + 4NO_2 + 2H_2O \quad [1]$$

$$SiO_2 + 6HF \rightarrow H_2SiF_6 + 2H_2O \quad [2]$$

Oxidants other than HNO_3 can also be used.

The actual reaction mechanism is quite complicated and involves many elementary reactions. Hydrogen and different oxides of nitrogen can evolve. Many rate equations for the dissolution of silicon wafer under different conditions have been proposed.[5-7]

Sometimes, the identification of the rate-controlling step in a heterogeneous process like this one (mass-transfer *vs.* reaction) becomes more critical than the knowledge of the actual chemistry in the design of an etcher, because a reaction-controlled etching requires a different design from a mass-transfer controlled etching to produce uniformly etched silicon wafers.

Schwartz and Robbins performed a series of experiments to quantify mass-transfer effects.[8] They etched wafers at different temperatures and correlated etch rates with the temperature using the Arrhenius expression. They attempted to identify the controlling step by the magnitude of the activation energy, a weak dependence of mass-transfer coefficient on temperature explained why the activation energy for the mass-transfer influenced (not controlled) etching was lower than that for the reaction influenced (not controlled) etching. This approach, although not very sophisticated, could be used to qualitatively recognize the rate-influencing step. Also, there is no quantitative evidence that kinetically controlled etching was achieved in these etching studies.

Bogenschütz *et al.,* however, claim that the viscosity of a liquid also can be expressed as an exponential function of temperature as follows[9]

$$\mu \propto e^{-Ea\mu/KT} \quad [3]$$

Since the viscosity is a transport property of the liquid, they claim that the temperature dependence of the viscosity is similar to the temperature dependence of mass-transfer rates. The argument is not entirely valid because the mass-transfer coefficient is a function of many temperature dependent parameters other than viscosity. However, it seems that it is an accepted approach to recognize that the rate-controlling step is based on the magnitude of the activation energy. This approach is useful for qualitative understanding of the etching process.

Robbins and Schwartz published a series of papers on acid etching of silicon from 1958 to 1976.[8,10-12] They essentially established that for low HF and high HNO_3 concentrations, the etching process is greatly influenced by diffusion. Even for the low nitric acid concentrations when the autocatalytic oxidation-reduction reaction influences the etching rate, mass-transfer effects are significant.[10,12] Their claim is supported by observations of Bogenschütz *et al.* and Klein and D'Stefan among many others.[9,13] Bogenschütz *et al.* showed that "activation energy" for mass-transfer controlled etching is comparable to the activation energy for viscosity.[9] Klein and D'Stefan observed a change in the etching rate with change in the mixing rate.[13] They observed a decrease in the dependence of the etching rate on the mixing rate with the increase in the HF concentration. This dependence was monotonic and linear. This means that the kinetic effects influence the etching process along with mass-transfer effects as the concentration of HF increases. Erk and Vandamme describe a process for chemical etching of silicon wafers where nitrogen bubbling is used for uniform mass-transfer effects.[14]

Various earlier as well as recent studies indicate a very strong transport effect on etching. However, often, the attempt to explain these effects is based on various kinetic mechanisms. Schimmel compared performances of different acid etches in defect decoration.[15] He gave a qualitative kinetic explanation for defect decoration based on local rate differentials. The effect of stirring and, hence, transport was reported to have a significant effect on the saturation current density of an n-type Si electrode.[16] A qualitative relationship between HF and/or oxidant concentration on the formation mechanism of stains in etching has been proposed by Nahm *et al.* and Schimmel and Elkind.[17,18] Fathauer *et al.* studied visible luminescence from silicon wafers subjected to etches producing stains.[19] Gaffney and Chiou observed that by reducing the etching rate and moving into dissolution-limited regions, staining of silicon in nitric-hydrofluoric-acetic acid system is reduced.[20] Bauer *et al.* recognized

* Electrochemical Society Member.
z E-mail: mkulkarni@memc.com

S0013-4651(99)02-063-7 CCC: $7.00

the importance of fluid mechanics in acid etching.[21] However, they gave no phenomenological explanation or quantification for the results observed. Studies in acid etching of materials other than silicon using HF have also reported the effect of HF concentration on the surface morphology of the etched substrate.[22] McAndrews and Sukanek postulate that in the device etching with HF, air bubbles may get trapped and cause surface irregularities.[23] However, they do not consider the possibility of formation of bubbles by the etching reaction or the resistance of these bubbles for the transport away from the attached sites. Performance of etching is a strong function of the equipment used as spray etching of silicon studied by John and Mcdonald seems to suggest.[24] This leads to the conclusion that mass-transfer effects are quite significant in acid etching, and many surface characteristics cannot be simply explained by studying chemical kinetics alone without taking transport effects into account. Thermodynamic dissolution windows for wet chemical processing of dilute aqueous Si-F system have been studied by Osseo-Asare *et al.,* but, the effect of molecular transport to the reaction sites still remained unanswered.[25] The shift in the controlling step, from kinetics to diffusion, in etching of thermal oxide by HF is discussed by Monk *et al.*[26,27] However, this study discusses only dissolution of thermal oxide by HF in a two-phase system. Monk *et al.* also reviewed chemical reaction mechanism and kinetics for hydrofluoric acid etching of silicon dioxide.[28] Kunii *et al.* studied wet etching of doped and nondoped silicon oxide films using buffered HF solution.[29] They observed that etch rate showed linear dependence on HF concentration at lower HF concentrations and nonlinear dependence on HF concentration at higher HF concentrations. This shift was explained by the change in the dominant reactive species. Nonuniformities in the oxide layer formed by boiling silicon wafers in HNO_3 were reported by Aoyama *et al.*[30] It is possible that nonuniformities may influence subsequent processing such as etching.

Many of the observations discussed above often lead to contradictory conclusions because effects of mass-transport were not well incorporated. The magnitude of the transport or diffusion effects is not only a function of the speed of transport given by a transport characteristic time or transport resistance, but also a function of the kinetic resistance or the kinetic characteristic time. The nature of the etched silicon wafer changes with a change in kinetic mechanism as well as transport properties. There has been no methodical investigation to quantify the relative impact of mass-transport effects and kinetic effects in the etching process. In acid-based etching the controlling mechanism can impart its signature on the etched surface. Also, previous attempts to quantify kinetic and mass-transfer effects in etching do not explain their effect on surface characteristics such as roughness and gloss.

The purpose of this study is to present our experimental data and analyze it using a novel phenomenological model for heterogeneous reactions. Data collected by us are consistent with the proposed phenomenological model for heterogeneous reactions and can explain various aspects of silicon surface characteristics. Since the proposed model explains different characteristics of the etched silicon wafer surface that earlier studies did not explain, there is a need for reporting this data and analysis in the public literature.

Phenomenological Model: Two-Phase System

The etching process itself typically involves the following steps (Fig. 1a): (*i*) transport of the reactants from the bulk solution to the wafer surface, (*ii*) effective reaction(s) on the wafer surface, and (*iii*) transport of products from the wafer surface to the bulk solution.

Reactants pass through a stagnant liquid film, which offers a finite resistance for mass-transfer before reactants reach the surface of the wafer. Products also pass through the mass-transfer film (henceforward, the term film refers to mass-transfer film unless specified otherwise). Hence, the reaction and physical transport of reagents occur as steps in series. The finite rate of chemical kinetics provides a finite kinetic resistance that acts in series with the mass-transfer resistance (Fig. 1a and b). When the mass-transfer and kinetic (reactive) resistances are comparable in magnitude, both kinetics and mass-transfer affect the rate of etching. However, when the difference in the kinetic and mass-transfer resistances is appreciable, the step with higher resistance controls the rate of acid etching. The phenomenological model shown in Fig. 1a and b is applicable to any typical solid-liquid system.

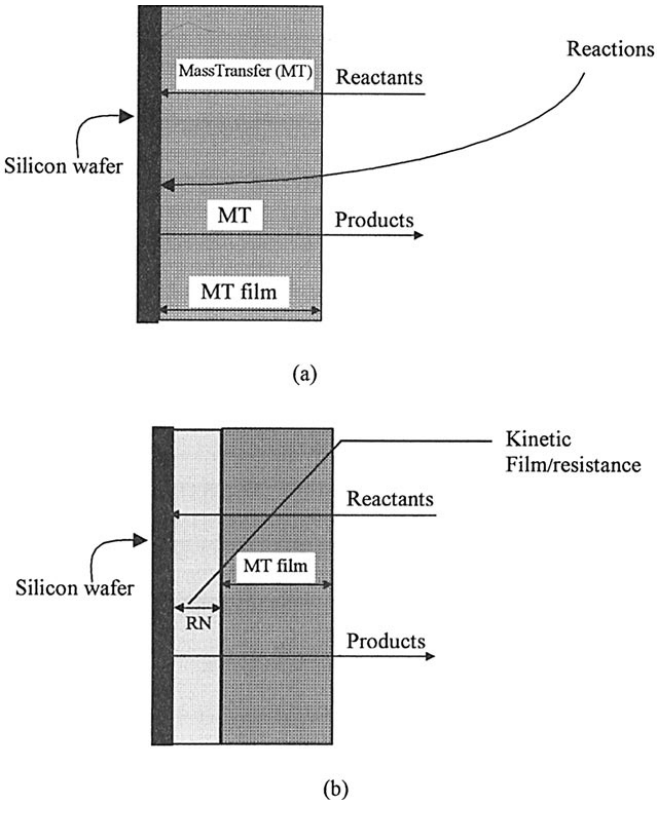

Figure 1. (a) A schematic representation of the mass-transfer resistance in a generic heterogeneous reaction system. (b) A phenomenological representation of the kinetic and mass-transfer resistances in a generic heterogeneous reaction system. (c) A phenomenological representation of the concentration boundary layer for the key reactant.

S0013-4651(99)02-063-7 CCC: $7.00

Kinetic (reactive) and transport resistances.—The two-phase phenomenological model proposed is shown in Fig. 1a and b. A finite mass-transfer resistance causes a drop in concentration of a species from the bulk value ($C_{b,i}$) to the solid-liquid interface value ($C_{f,i}$), and this drop is proportional to the mass-transfer resistance. According the classical mass-transfer theory,[31,32] the rate of transport across the mass-transfer film is given by

$$r_{m,i} = k_{m,i}(C_{b,i} - C_{f,i}) \quad [4a]$$

$$r_{m,i} = \frac{(C_{b,i} - C_{f,i})}{1/k_{m,i}} = \frac{DF_{m,i}}{R_{m,i}} \quad [4b]$$

where mass-transfer rates ($r_{m,i}$) are defined per cross-sectional area for transport for any given species i. All terms in equations are defined in the List of Symbols section. The driving force for the mass-transport is the concentration difference across the mass-transfer film, and the resistance to the transport is given by the inverse of mass-transfer coefficient.

The effective rate of reaction that incorporates adsorption-desorption-diffusion effects in the silicon wafer at the interface is given by

$$(r_{r,i}) = f_r(T, C_{f,i}, C_{f,j}...) \quad [5]$$

As an initial approximation, the effect of thermal boundary layer can be neglected; however, analysis of the model does not change if the thermal boundary layer effects are appreciable. Kinetic resistance for systems following simple kinetics is generally defined as a system constant.[31] Nonetheless, in this paper we extend this analysis and define a nonlinear kinetic resistance that varies as a function of interfacial species concentration

$$(R_{r,i}) = \frac{1}{\dfrac{f_r(T, C_{f,i}, C_{f,j}...)}{C_{f,i}}} \quad [6]$$

Using Eq. 6, Eq. 5 can be rewritten as

$$(r_{r,i}) = \frac{(C_{f,i} - 0)}{1/\dfrac{f_r(T, C_{f,i}, C_{f,j}...)}{C_{f,i}}} = \frac{DF_{r,i}}{R_{r,i}}$$

where reaction rates for any given species i ($r_{r,i}$) are defined per unit area where reaction takes place.

At steady state, at any given location, reaction rates are equal to mass-transfer rates ($r_{r,i} = r_{m,i}$). Thus, for any given system, and a given species, the kinetic and mass-transport resistances can be quantified and overall resistance is estimated as

$$r_i = \frac{DF_{o,i}}{R_{o,i}} = \frac{(C_{b,i} - 0)}{R_{o,i}} = \frac{(C_{b,i} - C_{f,i})}{R_{m,i}} = \frac{(C_{f,i} - 0)}{R_{r,i}}$$

$$\text{implies } R_{o,i} = R_{m,i} + R_{r,i} \quad [7]$$

Figure 1c shows the schematic picture of the proposed model.

Characteristic times.—The speed of a process is inversely proportional to its characteristic time. The speed of a process is also inversely proportional to the resistance of the process. Hence, characteristic time and the resistance of a given process are related to each other. For example, the resistances defined in Eq. 7 have units of seconds per meter. This means that the product of mass-transfer resistance with a characteristic length scale such as mass-transfer film thickness represents a characteristic time for mass-transfer. Similarly, the product of kinetic (reactive) resistance and a reaction length scale such as equivalent reaction film thickness represents a reaction characteristic time. Thus, for a special case when both reaction and mass-transfer length scales are identical (we can use thickness of either mass-transfer film or reactive film as the common length scale, provided both are of the same order of magnitude) the overall characteristic time of the process is given by summation of the characteristic kinetic time and characteristic transport time. Thus, as shown in Eq. 8, the resistance is a measure of the characteristic time

$$\tau_{m,i} = \delta_{m,i} \times R_{m,i} \quad \text{and} \quad \tau_{r,i} = \delta_{r,i} \times R_{r,i} \quad [8]$$

Application of resistances.—The influence of transport and kinetics on a system can be quantified by the ratio of mass-transport resistance to the kinetic resistance. If this ratio is greater than the critical minimum value (that is specific to a system) the system is mass-transport influenced. The system is kinetically controlled when this ratio is below its critical value

$$\frac{R_{m,i}}{R_{r,i}} > \left[\frac{R_{m,i}}{R_{r,i}}\right]_{min} \text{ implies mass-transport influenced}$$

and

$$\frac{R_{m,i}}{R_{r,i}} < \left[\frac{R_{m,i}}{R_{r,i}}\right]_{min} \text{ implies kinetically controlled} \quad [9]$$

Thus the system is either controlled by the dominant resistance or influenced by both when neither of the resistances is negligible.

One goal of etching is to reduce the surface roughness. Roughness is a measure of nonuniformity of the surface represented as a field of peaks and valleys (Fig. 2) and is defined as

$$\phi = \frac{\int_0^L \lambda dx}{\int_0^L dx} \quad [10]$$

where ϕ is the length averaged roughness. Note that λ is not a periodic function of x as Fig. 2 indicates for simplicity. Roughness can decrease only if the rate of removal (etching) at peaks ($r_{p,i}$) is greater than the rate of removal at valleys ($r_{v,i}$) such that

$$\frac{dh}{dt} = -\xi_{s-l}(r_{p,i} - r_{v,i}) = -(rl_p - rl_v) \quad [11]$$

where, ξ_{s-l} is the conversion factor that converts rates of consumption of species i per unit area, (r_i) to removal rates based on the decrease in thickness of silicon (rl). Based on the magnitude of mass-transport and kinetic resistances three cases can be studied.

Kinetically controlled etching.—As schematically explained in Fig. 3a, for acid-based etching, in the absence of a mass-transfer film, rates of removal at valleys and peaks are comparable ($rl_p \sim rl_v$). This is also the case when the mass-transfer film thickness is very low (Fig. 3b). This happens when the ratio of resistances is below the critical minimum value. Hence, kinetically controlled etching does not decrease roughness.

Mass-transfer influenced etching.—Mass-transfer influenced etching improves the surface roughness and gloss. Figure 3c explains the effect of mass-transfer film on the acid-based etching. The mass-transfer resistance is directly proportional to the thickness of the stagnant film. As shown in Fig. 3c, the mass-transfer resistance at the

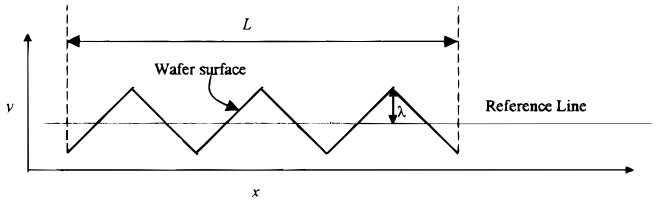

Figure 2. A schematic representation of roughness.

S0013-4651(99)02-063-7 CCC: $7.00

peaks is lower than that at valleys as a result of varying mass-transfer film thickness. Assuming that the kinetic resistance does not decrease significantly from peaks to valleys, the overall resistance is lower at peaks, and hence, removal rates at peaks are higher. As a result of preferential etching at peaks, reduction in roughness is observed. The ratio of etching rates at valleys and peaks is given by

$$\frac{r_{v,i}}{r_{p,i}} = \frac{rl_v}{rl_p} = \frac{R_{m,p,i}}{R_{m,v,i}} \frac{R_{r,p,i}}{R_{r,v,i}} \left[\frac{1 + \dfrac{R_{m,p,i}}{R_{r,p,i}}}{\dfrac{R_{m,p,i}}{R_{m,v,i}} + \dfrac{R_{m,p,i}}{R_{r,v,i}}} \right] < 1$$

$$\text{also } \frac{R_{m,p,i}}{R_{m,v,i}} < 1 \text{ that implies } \frac{rl_v}{rl_p} < 1 \quad [12]$$

Excessive mass-transfer controlled etching.—If the mass-transfer film thickness is very low, the kinetic effects become stronger and etching tends to be kinetically controlled. If the mass-transfer film is very thick, although mass-transport effects are predominant, the relative difference between the film thickness at peaks and valleys decreases as the total film thickness increases, *i.e.*

when

$$\lim_{\delta_{m,p,i}, \delta_{m,v,i} \to \infty} \left[\frac{R_{m,p,i}}{R_{m,v,i}} \right] = 1 \text{ implies } \lim_{\delta_{m,p,i}, \delta_{m,v,i} \to \infty} \left[\frac{r_{v,i}}{r_{p,i}} \right] = 1$$

then

$$\lim_{\delta_{m,p,i}, \delta_{m,v,i} \to \infty} \left[\frac{R_{m,i}}{R_{r,i}} \right] > \left[\frac{R_{m,i}}{R_{r,i}} \right]_{max} \quad [13]$$

where $[R_{m,i}/R_{r,i}]_{max}$ is the critical excessive (maximum) resistance ratio and is specific to a system. Thus, simply increasing mass-transport resistance does not decrease the roughness. There is an optimum thickness of the mass-transfer film for each process. This optimum level is obtained when difference between etching rates at peaks and valleys reaches the maximum.

Quantification of polishing efficiency.—Instantaneous polishing efficiency is defined as the ratio of actual rate of polishing to the maximum possible rate of polishing, *i.e.,* it is equal to the ratio of difference between the etching rates at peaks and valleys to the etching rate only at peaks

$$\eta_{pol,inst} = \frac{-\left(\dfrac{dh}{dt}\right)}{-\left(\dfrac{dh}{dt}\right)_{max}} = \frac{rl_p - rl_v}{rl_p}$$

$$= 1 - \frac{R_{m,p,i}}{R_{m,v,i}} \frac{R_{r,p,i}}{R_{r,v,i}} \left[\frac{1 + \dfrac{R_{m,p,i}}{R_{r,p,i}}}{\dfrac{R_{m,p,i}}{R_{m,v,i}} + \dfrac{R_{m,p,i}}{R_{r,v,i}}} \right] \quad [14a]$$

The average polishing efficiency is the integral average of the instantaneous polishing efficiency and is calculated as follows

$$\eta_{pol,avg} = \frac{\displaystyle\int_{h_1}^{h_2} \eta_{pol,inst} dh}{\displaystyle\int_{h_1}^{h_2} dh} = \frac{\displaystyle\int_{h_1}^{h_2} \left[-\left(\frac{dh}{dt}\right) \Big/ -\left(\frac{dh}{dt}\right)_{max} \right] dh}{\displaystyle\int_{h_1}^{h_2} dh}$$

$$= \frac{\displaystyle\int_{h_1}^{h_2} \frac{rl_p - rl_v}{rl_p} dh}{\displaystyle\int_{h_1}^{h_2} dh} \quad [14b]$$

Thus, the average polishing efficiency is a function of surface kinetics and mass transport. For simple case of a first order kinetics and a

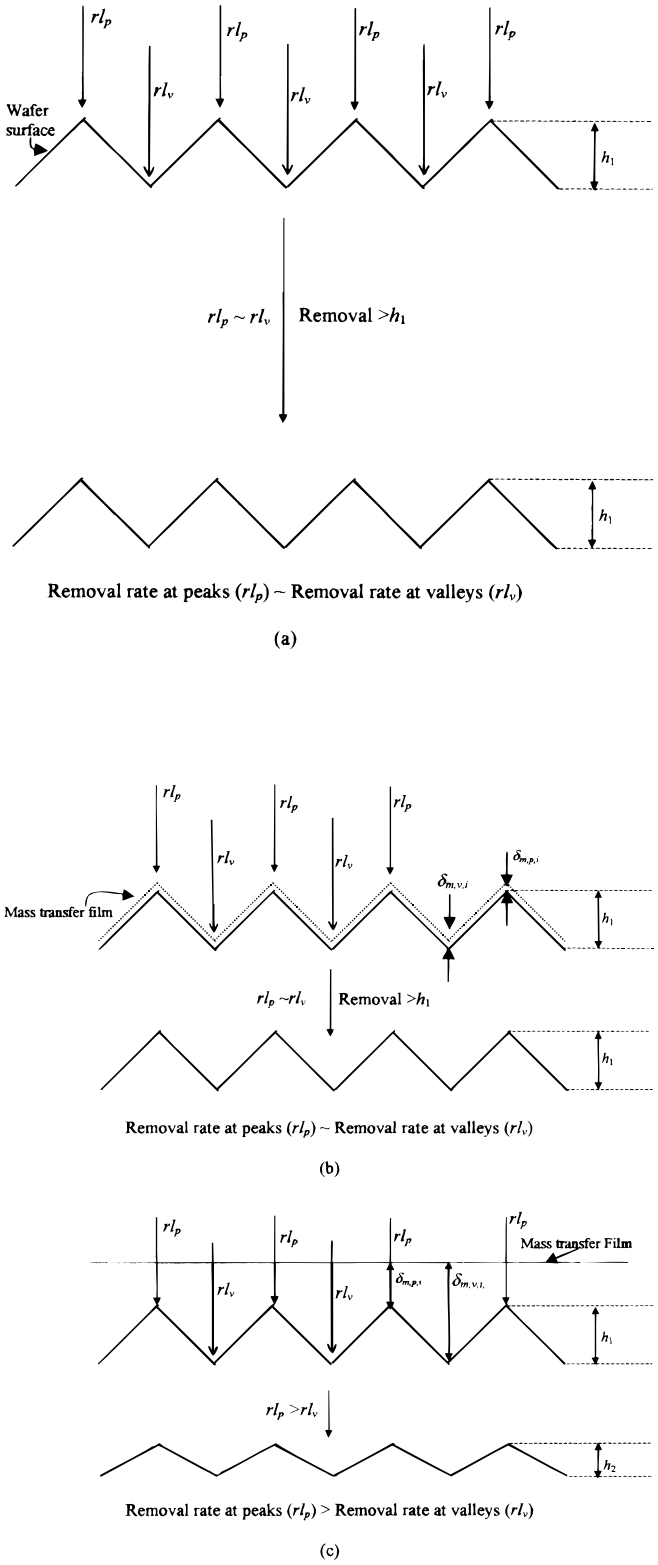

Figure 3. (a) A schematic speculation about a kinetically controlled etching process. (b) A schematic view of insufficient mass-transfer effects on the etching process. (c). A schematic view of sufficient mass-transfer effects on the etching process.

S0013-4651(99)02-063-7 CCC: $7.00

fixed mass-transfer film thickness, the average polishing efficiency to achieve a completely flat surface is derived by solving Eq. 14b as

$$\eta_{pol,avg} = \frac{\dfrac{h_1}{\delta_{m,v,i}}}{2\left(1 + \dfrac{R_{r,i}}{R_{m,v,i}}\right)} \text{ for } \delta_{m,v,i} \geq h_1, \text{ and } h_2 = 0 \quad [15]$$

However, numerical estimation of polishing efficiency may become necessary for a more complex etching kinetics.

Thus, the mass-transfer film must be thick enough such that the ratio of mass-transfer resistance to kinetic resistance must be above the critical minimum resistance ratio to ensure sufficient mass-transfer influence; also, the mass-transfer film must be thin enough such that the ratio of rate of etching at peaks to that at valleys is greater than unity. The dependence of polishing efficiency on the ratios of these resistances is schematically shown in Fig. 4. The polishing efficiency gradually increases with increasing ratio of mass-transfer resistance to kinetic resistance, reaches a maximum value, and then asymptotically approaches zero. Change in roughness to removal ($-\Delta\Phi/\Delta Y$) ratio is higher for a higher polishing efficiency.

Phenomenological Model: Three-Phase System

Acid etching of silicon wafers is greatly influenced by gaseous products. In the phenomenological model presented in the previous section, the effect of gaseous products on the etching rate was not addressed. Macromodeling of etching must incorporate (*i*) transport of the reactants in the liquid phase from the bulk solution to the wafer surface, (*ii*) effective reaction(s) on the wafer surface to produce products in both liquid and gas phase, (*iii*) detachment of gaseous products (bubbles) from the silicon surface, and (*iv*) transport of the gaseous products (bubbles) to the bulk phase.

NO_x and hydrogen are generated by the etching reaction. These gases form bubbles that adhere to the silicon surface for a finite period of time before they are dislodged. The etching reaction cannot take place on the sites masked by bubbles. Since the effective local thickness of the mass-transfer film is also affected by the dislodged bubbles moving in this film, the rate of etching is affected by dislodged bubbles as well. The masking effect of bubbles influences the overall rate of etching and also affects the surface morphology. However, the bubble masking effect could be partially reduced by reduction in mass-transfer resistance resulting from the mixing caused by the detached bubbles in the mass-transfer film (autoreduction of bubble masking).

Figure 5a shows a schematic of the silicon surface at any time during an etching process. The wafer surface is randomly covered by the bubbles produced by the reaction. Thus, at any instant, a fraction of the silicon wafer surface is masked by the bubbles and the rest is covered by the liquid mass-transfer film. A site on the wafer surface is randomly occupied by gas and liquid alternately. This three-phase system is modeled as shown in Fig. 5b. The energy required to detach a bubble from the silicon surface depends on the surface tension, viscosity, density, and the surface structure (roughness) among many other dynamic and thermodynamic parameters. Therefore, estimation of the energy required to dislodge the bubbles from the silicon surface requires a rigorous experimental approach. The effect of the bubbles covering the silicon surface is incorporated by the bubble detachment resistance which is a measure of difficulty involved in dislodging the bubbles from the silicon surface. The detached bubbles face the film bubble transport resistance in the mass transport film before entering the liquid bulk. The cumulative effects of the bubble detachment resistance and the film bubble transport resistance are given by the overall bubble transport resistance. Henceforth, for simplicity, this overall bubble transport resistance is referred to as the bubble transport resistance. Since the bubbles on the silicon wafer as well as the bubbles in the mass-transfer film contribute to the bubble masking effect, the bubble transport resistance describes a more complete effect of the bubbles. Since the bubbles occupy a fraction of the silicon wafer and influence the effective transport rate of liquid-phase reactants, the overall etching rate is also affected. Our model assumes that the bubble transport resistance and liquid-phase mass-transport resistance act in parallel, since both the bubbles and the liquid-phase occupy the silicon surface simultaneously. For engineering application, these two resistances are lumped together as the effective liquid-phase mass-transport resistance or simply effective mass-transport resistance as shown in Fig. 5b. Since the kinetic resistance and the effective mass-transport resistance act in series, the overall resistance is given as

$$R_{o,i} = R_{r,i} + \frac{R_{m,g}R_{m,i}}{R_{m,g} + R_{m,i}} = R_{r,i} + R_{m,eff,i} \quad [16]$$

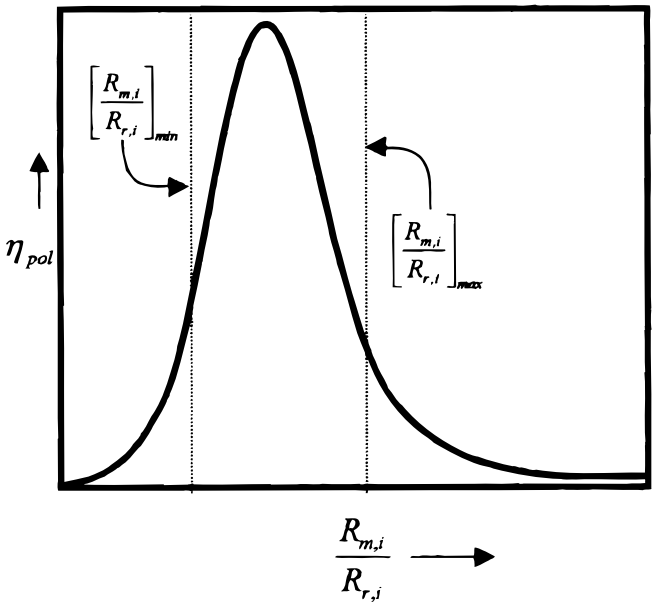

Figure 4. Dependence of polishing efficiency on the ratio of mass-transfer resistance to the kinetic resistance.

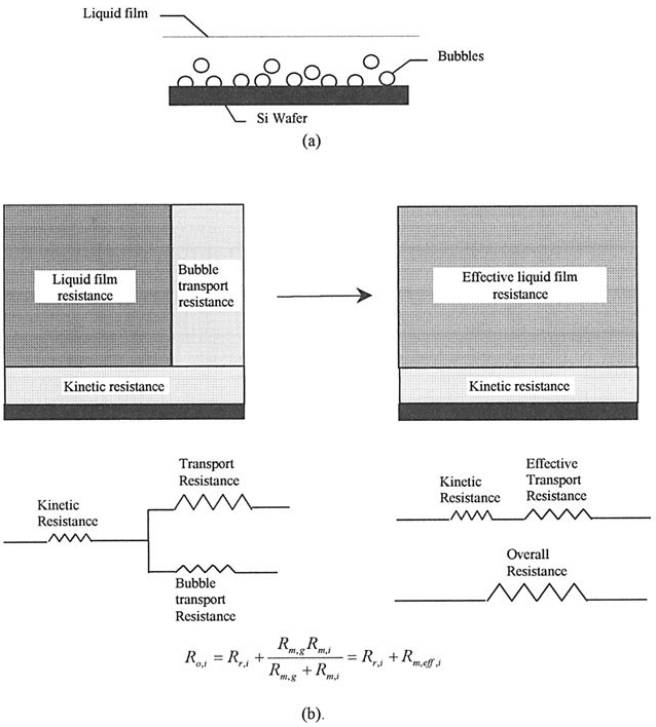

Figure 5. (a) A schematic representation of the three-phase etching process. (b) A phenomenological representation of resistances in series and parallel.

S0013-4651(99)02-063-7 CCC: $7.00

On a macroscale, analysis for the two-phase system now can be extended to the three-phase system. As in the case of the two-phase system, the roughness for the three-phase system can be characterized using Eq. 9 through 15 using the effective liquid-phase resistance ($R_{m,eff,i}$) and kinetic resistance ($R_{r,i}$). $R_{m,eff,i}$ is determined experimentally by measuring the etching rates and following the same analysis as for the two-phase system.

Effect of bubbles on silicon surface.—As discussed earlier, the etching reaction produces gaseous products that form the bubbles that adhere to the surface. If the bubbles adhere on a site for an appreciable period of time, the site covered by bubbles can form a peak as surrounding sites are continuously etched. A schematic of the effect of bubbles on a smooth surface is shown in Fig. 6a and b.

The characteristic bubble formation time or bubble formation resistance is a function of the characteristic kinetic time or kinetic resistance for a given species i. Characteristic bubble transport time or the bubble transport resistance is a nonlinear function of the viscosity, surface tension, hydrodynamics, and silicon surface itself. If the ratio of the bubble transport resistance to bubble formation resistance is greater than the critical bubble masking resistance ratio that is specific to a system, etching produces an uneven surface with peaks resulting from the bubble masking effect. This happens when the bubbles formed on the surface stay there long enough to cause an appreciable difference in the removal between masked and unmasked sites. When the ratio of bubble transport resistance to bubble formation resistance is smaller than this critical ratio, there is a negligible masking effect, *i.e.,* the bubbles are dislodged from the surface before there is appreciable difference in removal between the masked and unmasked sites. The bubble masking effect is a continuous function of the ratio of the bubble transport resistance to bubble formation resistance, *i.e.,* the masking effect gradually increases with increasing ratio of these resistances. Moreover, the critical value of this ratio can be defined based on the acceptable roughness as required by the specifications. Thus

$$\frac{R_{m,g}}{R_{r,i}} > \left[\frac{R_{m,g}}{R_{r,i}}\right]_{bm} \quad \text{implies Bubble masking}$$

$$\text{and } \frac{R_{m,g}}{R_{r,i}} < \left[\frac{R_{m,g}}{R_{r,i}}\right]_{bm} \quad \text{implies No bubble masking} \quad [17a]$$

Since the cumulative effects of bubble transport resistance and liquid-phase resistance for the key species are given by an effective liquid-phase mass-transport resistance for the key species (Eq. 16), Eq. 17a is expressed as

$$\frac{R_{m,eff,i}}{R_{r,i}} > \left[\frac{R_{m,eff,i}}{R_{r,i}}\right]_{bm} \quad \text{implies masking}$$

$$\text{and } \frac{R_{m,eff,i}}{R_{r,i}} < \left[\frac{R_{m,eff,i}}{R_{r,i}}\right]_{bm} \quad \text{implies no masking} \quad [17b]$$

A more detailed relationship can be correlated by collecting experimental data to relate a surface character to the ratio of these resistances as follows

$$SC = f_{sc}\left(\frac{R_{m,eff,i}}{R_{r,i}}\right) \quad [18]$$

where *SC* can be roughness or any other surface character affected by resistances (such as gloss which is discussed in the Appendix). Equations 17b and 18 require parameters that can be experimentally estimated.

The effective resistances thus defined are used to describe the three-phase system as a pseudo two-phase system discussed in the previous section. For example, Eq. 12 that defines the ratio of the rate of removal at valleys to that at peaks for the two-phase system is now defined as

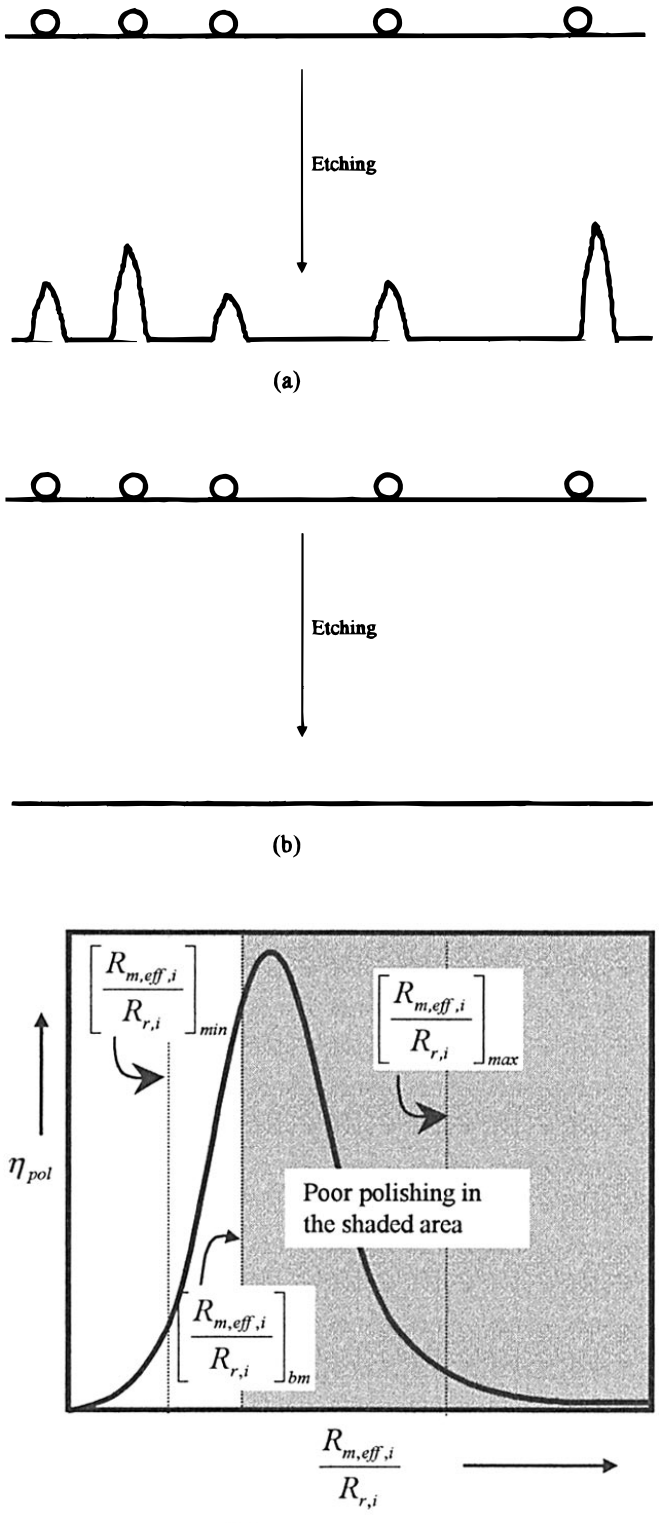

Figure 6. (a) Effect of bubble masking on the surface for $R_{m,eff,i}/R_{r,i} > R_{m,eff,i}/R_{r,i}|_{bm}$. (b) Effect of bubble masking on the surface for $R_{m,eff,i}/R_{r,i} < R_{m,eff,i}/R_{r,i}|_{bm}$ (c). Dependence of polishing efficiency on the ratio of the effective mass-transfer resistance to the kinetic resistance. (Solid line indicates η_{pol} in the absence of bubble masking.)

S0013-4651(99)02-063-7 CCC: $7.00

$$\frac{r_{v,i}}{r_{p,i}} = \frac{rl_v}{rl_v} = \frac{R_{m,eff,p,i}}{R_{m,eff,v,i}} \frac{R_{r,p,i}}{R_{r,v,i}} \left[\frac{1 + \frac{R_{m,eff,p,i}}{R_{r,p,i}}}{\frac{R_{m,eff,p,i}}{R_{m,eff,v,i}} + \frac{R_{m,eff,p,i}}{R_{r,v,i}}} \right]$$

$$< 1 \text{ since } \frac{R_{m,p,i}}{R_{m,v,i}} < 1 \quad [19]$$

Equations 13-15 are derived in a similar fashion for the three-phase system. By using the effective resistances, the three-phase system is analyzed analogous to the two-phase system at a macroscale.

Dependence of the polishing efficiency on the ratio of effective mass-transfer resistance to the kinetic resistance is schematically shown in Fig. 6c. The relationship between the change in roughness to removal ($-\Delta\Phi/\Delta Y$) ratios and $R_{m,eff,i}/R_{r,i}$ is similar to that in the case of the two-phase system. The difference is that in the case of three-phase system, polishing efficiency decreases because of bubble masking effect.

Experimental

The above phenomenological model was proposed using classical chemical engineering fundamentals to explain experimental data collected under various conditions. In this study we discuss the nature of these experiments and qualitatively analyze collected data using the proposed phenomenological model.

Experiments were conducted in two different setups. Most of the experiments were performed using the setup shown in Fig. 7a.[14] Etchant acid is fed into the etcher along with optional nitrogen gas at a high pressure. Nitrogen, when optionally introduced, remains well mixed in the liquid and is partly in the form of bubbles. A process box containing silicon wafers is placed in the etcher as shown in Fig. 7a. The process box hosts an assembly of rotors that rotate the wafers about their centers. Silicon wafers were etched at different concentrations and temperatures and the data collected were analyzed using the three-phase phenomenological model.

Another experimental setup shown in Fig. 7b was also used for a few single wafer experiments. In a bath of acid mixture, a single wafer can be etched at different rotational speeds. The arrangement involves mounting the back surface of the wafer to a rotating disk. The glue used to mount the wafer was attacked by the acid and some flakes of glue residue were added to the acid causing some masking effects. Hence, in this setup, the surface of the wafer was influenced by the glue holding the wafer and rotating disk together.

Results and Discussion

Effect of bubbles.—Intrinsic bubbles.—The gas bubbles produced by the etching reaction (hydrogen + NO_x) are referred to as the intrinsic bubbles. The effect of these intrinsic bubbles on the surface morphology is better understood by studying surface profile. Surface irregularities are also observed by using optical inspection techniques that identify peaks and valleys on the basis of intensity of reflected light. One such technique involves generation of light scatter picture (LSP) where the peaks and valleys on the surface are captured as spots of varying intensity (Fig. 8).

Surface profile of a smooth polished silicon wafer is shown in Fig. 9a. As can be observed in this figure, there are no surface irregularities detected within the resolution of the equipment. LSP (Fig. 9b) of a polished wafer shows no surface irregularities. These polished wafers were then etched at 5 rpm in a mixture of HF + HNO_3 + H_3PO_4. The surface profile and LSP of the etched wafer are shown in Fig. 10a and b, respectively. It is apparent that the surface irregularities are caused by the bubbles formed on the surface. Since wafer rotation speed was very low, the effective mass-transfer resistance was high (effective mass-transfer coefficient was low), *i.e.,* $R_{m,eff,i}/R_{r,i} > (R_{m,eff,i}/R_{r,i})_{bm}$. Hence, the bubble masking effect produced peaks during etching and resulted in a rougher surface. Moreover, to support this argument, it is necessary to show that when $R_{m,eff,i}/R_{r,i} < (R_{m,eff,i}/R_{r,i})_{bm}$, surface irregularities are negligible. This

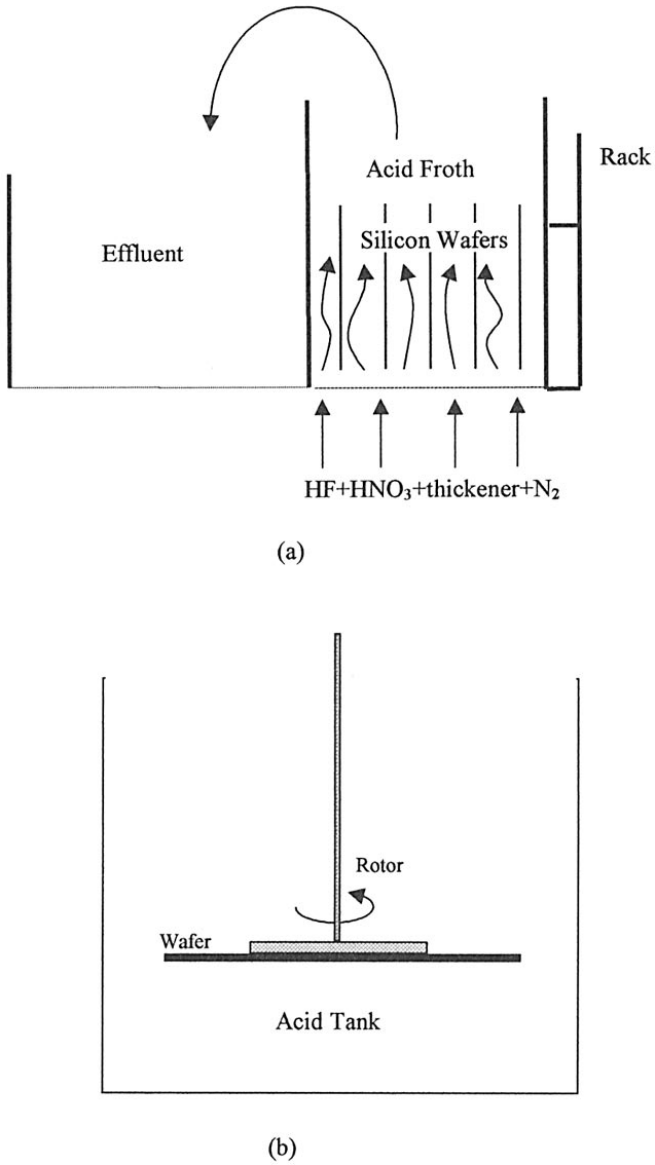

Figure 7. (a) The experimental assembly to etch silicon wafers. (b) The experimental setup for single wafer etching at different rotational speeds.

can be achieved by etching wafers at a lower $R_{m,eff,i}$. The mass-transfer resistance decreases with increasing mixing intensity or surface shear. The surface shear as well as the mixing intensity is increased by increasing the wafer rotational speed. Hence, silicon wafers were etched at 60 rpm in the same acid mixture and results of this experiment are shown in Fig. 11a and b. Surface contour (Fig. 11a) shows negligible irregularity and the LSP of the etched wafer shows a very smooth surface. An increase in the rotation speed affects the mass-transfer resistance. At higher rotation speeds, the mass-transfer resis-

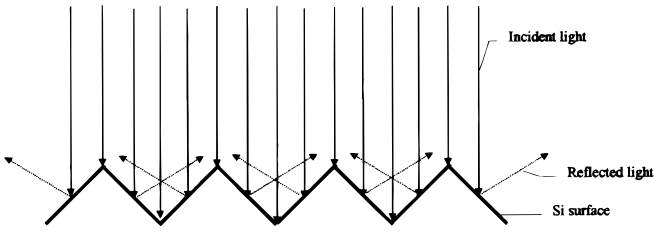

Figure 8. A schematic picture of LSP (light scatter picture).

S0013-4651(99)02-063-7 CCC: $7.00

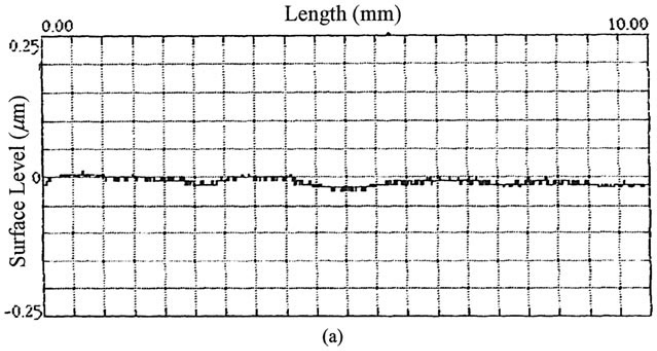

(a)

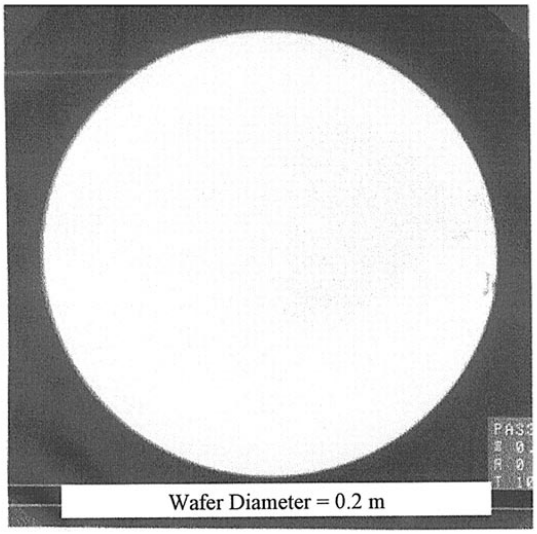

(b)

Figure 9. (a) Surface profile of a smooth polished wafer. (b) LSP of a smooth polished silicon wafer.

tance is lower and, hence, $R_{m,eff,i}/R_{r,i} < [R_{m,eff,i}/R_{r,i}]_{bm}$. Thus, at high rotational speed, the etched wafers showed smoother surface and minimal bubble masking effect.

The mass-transfer resistance decreases with increasing mixing intensity. To clearly demonstrate the influence of the effective mass-transfer resistance on the bubble masking effect and the effect of bubble masking on surface irregularities, a simple experiment was performed using the laboratory scale setup described in Fig. 7b. A polished silicon wafer was etched in a very dilute etching mixture (with negligible molar HF concentration), in the horizontal position. The effect of gravity and the orientation of the silicon wafer increased the bubble transport resistance ($R_{m,g}$). The wafer was etched for more than 15 μm removal, at 60 rpm. The LSP (Fig. 12a), and surface profile at the center (Fig. 12b) and at periphery (Fig. 12c) clearly show the influence of the effective mass-transfer resistance on the bubble masking. Shear and the centrifugal force at the center of the wafer were lower than the shear and the centrifugal force at the periphery (Levich's solution is not applicable here).[33] The bubble masking resistance decreased with increasing radial distance from the center. The effective mass-transfer resistance at the center was higher than the mass-transfer resistance at the periphery of the wafer. Thus, the bubble masking effect was predominant in the central region of the wafer where $R_{m,eff,i}/R_{r,i} > [R_{m,eff,i}/R_{r,i}]_{bm}$; $R_{m,eff,i}$ decreased along the radius, and hence, the bubble masking effect decreased along the radius, which is shown by the smoother surface at the periphery (Fig. 12b and c) where $R_{m,eff,i}/R_{r,i} < [R_{m,eff,i}/R_{r,i}]_{bm}$. These surface irregularities are referred to in literature as the orange peel.

Extrinsic bubbles.—In the industrial etcher (Fig. 7a) nitrogen bubbling can be used to achieve a more homogeneous turbulence to improve the performance. The bubbles generated by sparging or the introduction of an inert gas into the etch-bath are referred to as the extrinsic bubbles. This extrinsic bubbling also leaves its signature on the etched surface. The smooth polished wafers show a wavy pattern after etching under extrinsic bubbling (Fig. 13a and b). However, extrinsic bubbles impart waviness of lower frequency. The extrinsic bubbles increase the mixing intensity and decrease the bubble masking and effective mass-transfer resistances. Hence, the extrinsic bubbles help reduce surface roughness by decreasing the bubble transport resistance. However, very intense gas sparging is not advisable because it may either lead to kinetically influenced conditions by decreasing the effective mass-transfer resistance or lead to a drop in etching rates by excessive extrinsic bubble coverage.

Figure 14 shows the effect of extrinsic bubbling on the surface roughness. Rough silicon wafers with very low gloss (0-5 gloss units) and high ϕ (0.2-0.3 μm) were etched with and without extrinsic nitrogen bubbling in a 1.5 M HF + 1.5 M H_3PO_4 + excess HNO_3 mixture. Improvement in the roughness was very poor when the intrinsic bubble masking effect was present, *i.e.,* when $R_{m,g}$ was higher. $R_{m,g}$ is lower when the extrinsic bubbling is present, and hence, polishing efficiency and reduction in roughness were higher in the presence of the extrinsic bubbling. Thus, roughness of etched silicon wafers etched under different hydrodynamic conditions can be explained by the proposed phenomenological model.

Effect of overall mass-transfer.—A series of experiments was performed using the setup described in Fig. 7a to establish the effect of mass-transport on improvement in roughness of etched wafers. The experiments were conducted with and without the viscous thickener (H_3PO_4) at various HF concentrations and at different tempera-

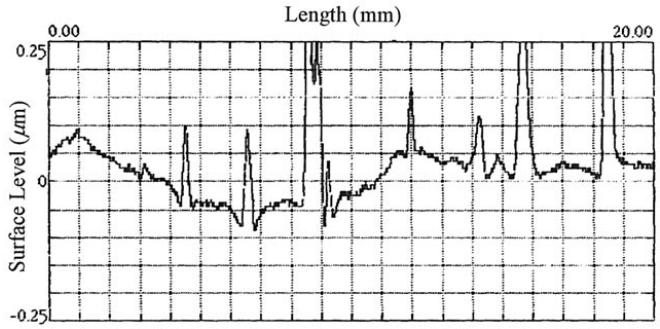

(a)

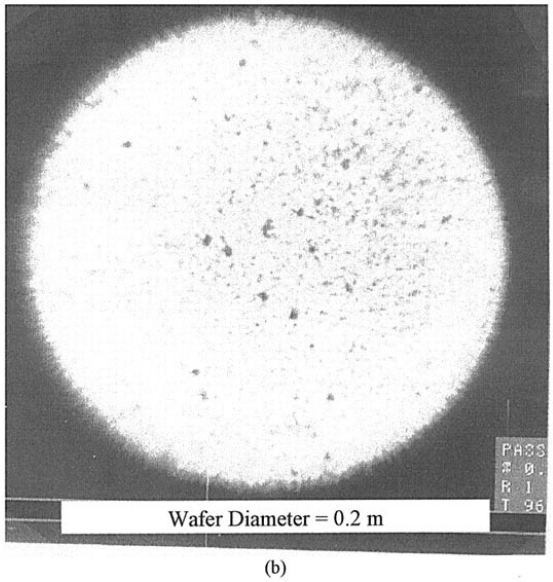

(b)

Figure 10. (a) Surface profile of a wafer etched at 5 rpm with no extrinsic bubbling. (b) LSP of a wafer etched at 5 rpm with no extrinsic bubbling.

S0013-4651(99)02-063-7 CCC: $7.00

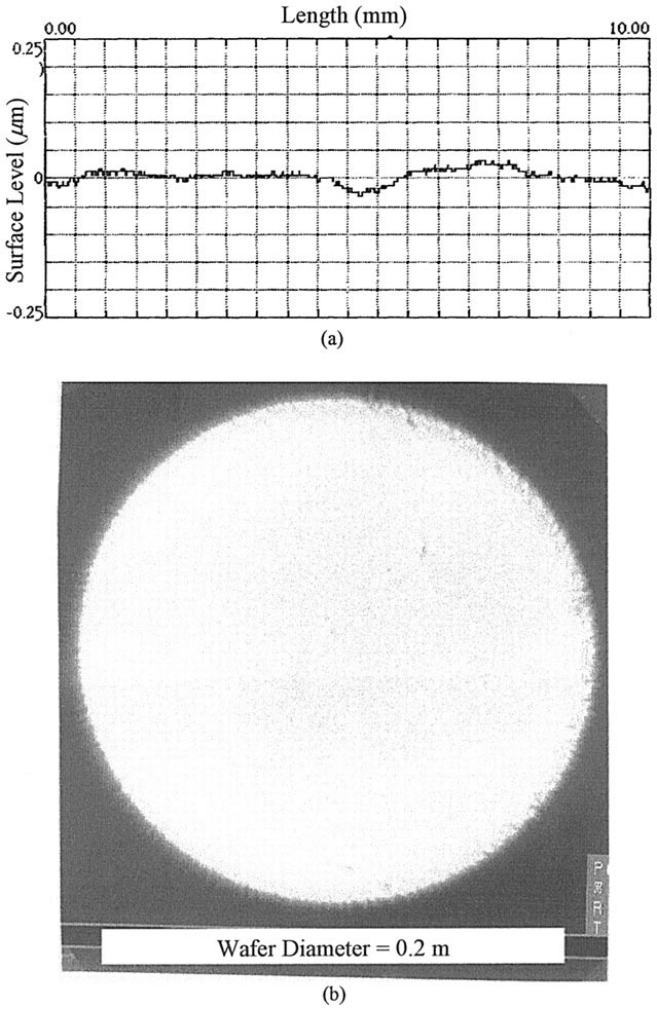

Figure 11. (a) Surface profile of a wafer etched at 60 rpm with no extrinsic bubbling. (b) LSP of a wafer etched at 60 rpm with no extrinsic bubbling.

tures with wafers rotating at 6 rpm and at approximately 6×10^5 Pa upstream nitrogen pressure. Rough silicon wafers with very low gloss (0-5 gloss units) and high ϕ (0.2-0.3 μm) were etched in all experiments discussed below.

Effect of thickener.—A mixture of HF and HNO_3 has density and viscosity closer to those of water. Hence, the mass-transfer resistance or the thickness of the effective transport-film for such a mixture can be quite low. Addition of a thick viscous acid to this mixture, which does not chemically participate in the etching reaction should not alter the chemical kinetics, but should increase the mass-transfer resistance as a result of the increase in the viscosity, *i.e.,* $\partial(k_{m,eff,HF})/\partial\mu < 0$ implies $\partial(R_{m,eff,HF})/\partial\mu > 0$ implies $\partial(R_{m,eff,HF})/\partial C_{b,thk} > 0$. Since the bulk viscosity increases with concentration of the thickener, the effective mass-transfer resistance increases with the concentration of the thickener.

In the industry, it has been observed that addition of a few viscous acids to the mixture of HF and HNO_3 decreases the roughness of the wafer more efficiently for the same removal. As discussed earlier, addition of a thickener increases the effective mass-transfer resistance ($R_{m,eff,HF}$). Thus, $R_{m,eff,HF}/R_{r,HF}$ increases with the thickener concentration, *i.e.,* $\partial(R_{m,eff,HF}/R_{r,HF})/\partial C_{b,thk} > 0$. It follows from Eq. 14 and 19 that the ratio of change in roughness to removal improves with increasing difference between the removal rates at peaks and valleys. This difference increases with increasing mass-transfer effects if thickness of the mass-transfer film is below the optimum (Fig. 4 and 6c). Thus, increasing concentration of the thickener must increase the polishing efficiency, *i.e.,* roughness to removal ratio ($-\Delta\Phi/\Delta Y$), must also improve. Figure 15 shows the effect of the thickener concentration on the roughness to removal ratio. It is clearly observed that the

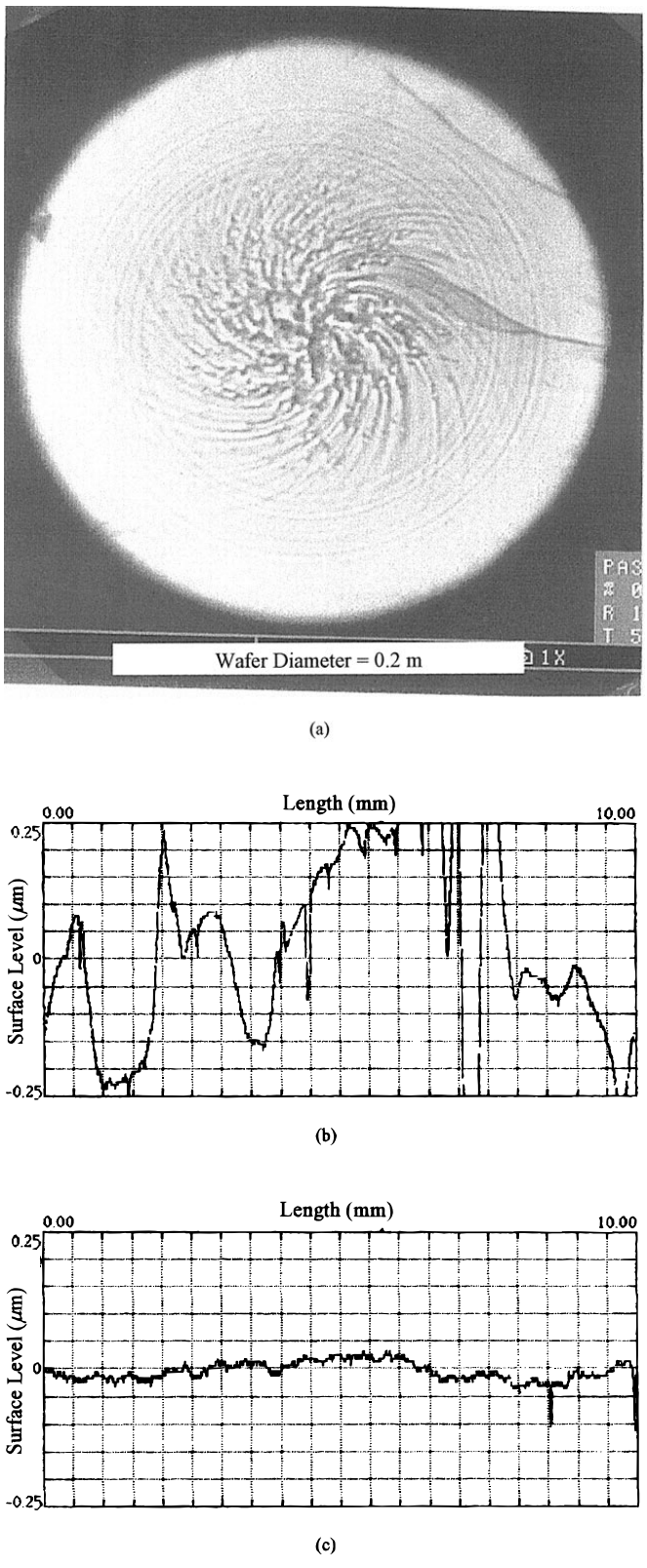

Figure 12. (a) LSP of a wafer etched at 60 rpm and at a lower HF concentration. (b). Central surface profile of a wafer etched at 60 rpm and at a lower HF concentration. (c). Peripheral surface profile of a wafer etched at 60 rpm and a lower HF concentration.

S0013-4651(99)02-063-7 CCC: $7.00

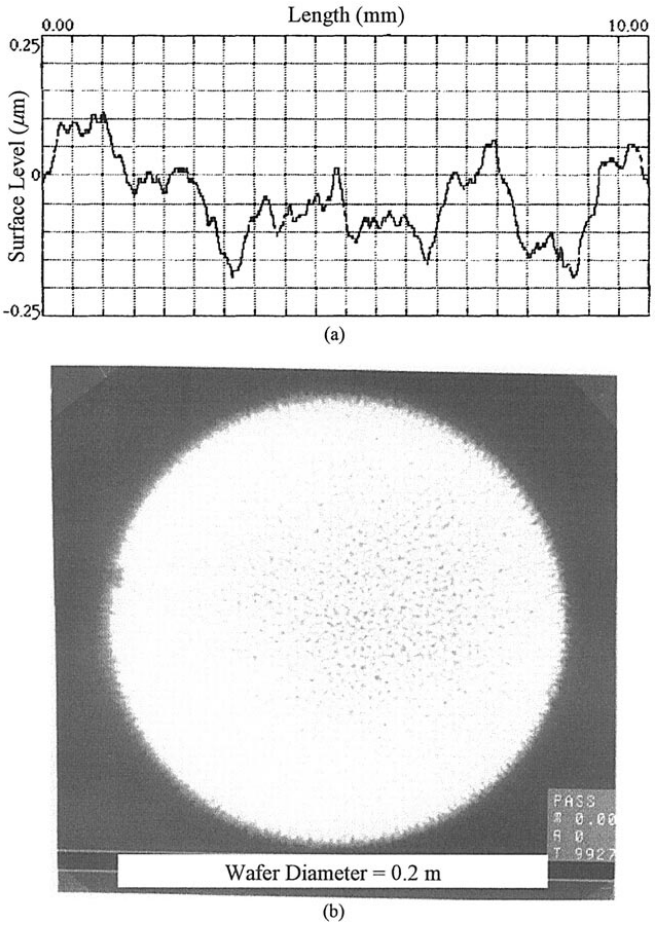

Figure 13. (a) Surface profile of a wafer etched with extrinsic nitrogen bubbling. (b) LSP of a wafer etched with extrinsic nitrogen bubbling.

thickener influences the mass-transfer effects of etching and decreases roughness.

Effect of HF concentration.—Mixed acid used in etching has excess HNO_3. In many cases, molar ratio of HF:HNO_3 in the etching mixture varies from 1:10 to 1:5. Since nitric acid is in abundance, the relative concentration of nitric acid does not vary appreciably during etching. Thus, HF becomes the rate influencing reactant. Hence, chemical kinetics is primarily dependent on the concentration of HF. The etching rate increases with an increase in the HF concentration. The dependence of the kinetic rate on the HF concentration can be applied to define the kinetic resistance as

$$r_{r,HF} = \frac{f_r(T,\ C_{f,i},\ C_{f,j},...C_{f,HF})}{C_{f,HF}}(C_{f,HF} - 0) = \frac{(C_{f,HF} - 0)}{R_{r,HF}} \quad [20]$$

The kinetic resistance is a function of the temperature and interfacial concentration of reactants. $R_{r,HF}$ can decrease, increase, or remain unchanged in response to a change in interfacial, and hence, bulk HF concentration.

The mass-transfer resistance, $R_{m,eff,HF} = 1/k_{m,eff,HF}$ is not a strong function of HF concentration (it is assumed that mass-transfer coefficient does not vary appreciably with concentration of a species if changes in density and viscosity are negligible). Hence, by varying concentration of the key reactant HF, the ratio of the effective mass-transfer resistance to the kinetic resistance, $R_{m,eff,HF}/R_{r,HF}$, can be varied. Since this ratio dictates the relative effect of mass-transport over kinetics, the polishing efficiency, and change in roughness to removal ratio, $(-\Delta\Phi/\Delta Y)$ can be varied by varying the HF concentration. Expressed mathematically

$$\frac{\partial\left(\frac{R_{m,eff,HF}}{R_{r,HF}}\right)}{\partial C_{b,HF}} \neq 0 \text{ implies } \frac{\partial \eta_{pol}}{\partial C_{b,HF}} \neq 0 \quad [21]$$

Figure 16 shows dependence of roughness on the HF concentration at different thickener concentrations. Experimental data indicates that $-\Delta\Phi/\Delta Y$ increases with the increasing HF concentration. Hence, the polishing efficiency improves with increasing HF concentration. Figure 17 shows improvement in $-\Delta\Phi/\Delta Y$, and hence, in polishing efficiency with increasing HF concentration. These results indicate the dependence of the kinetic resistance on HF concentration, *i.e.,* $R_{m,eff,HF}/R_{r,HF}$ is sensitive to changes in the HF concentration. Since the mass-transfer resistance does not change appreciably with the HF concentration, it follows from Eq. 20 and 21 that the

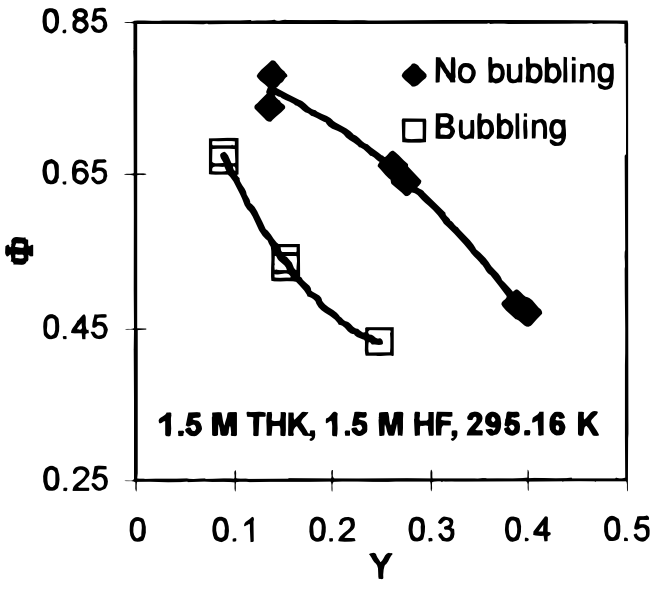

Figure 14. Effect of extrinsic bubbling on roughness.

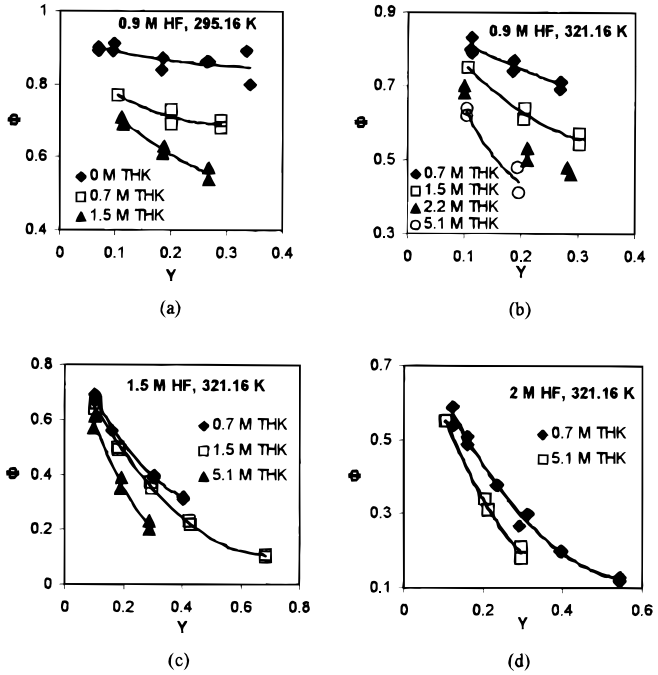

Figure 15. Effect of the thickener concentration on roughness at a constant HF concentration.

S0013-4651(99)02-063-7 CCC: $7.00

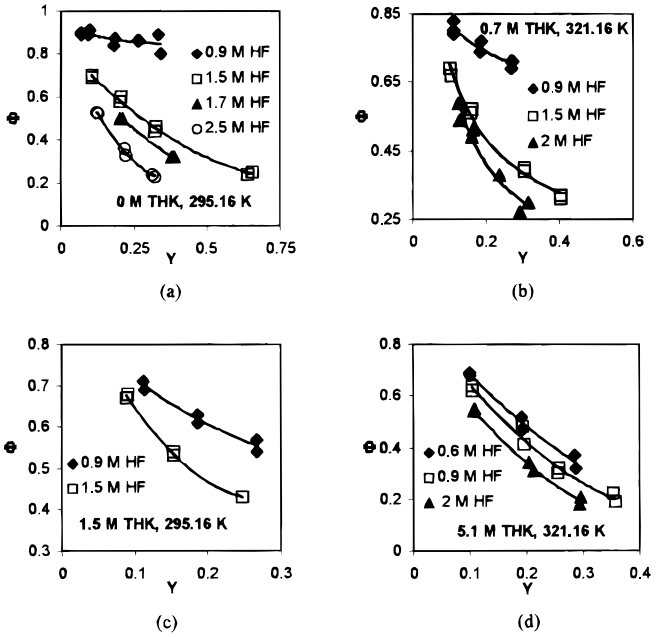

Figure 16. Effect of HF concentration on roughness at a constant thickener concentration.

kinetic resistance changes with HF concentration. It also implies that the kinetic rate is a stronger function of HF concentration than the mass-transfer rate is. Thus, the HF concentration can be increased to improve polishing efficiency. However, at higher HF concentrations etching rates are uncontrollably high, and process control and runaway become a concern. The etching reaction is exothermic in nature, and hence, at high removal rates, the heat generation rate can easily exceed the heat removal rate by plastic heat exchangers which must be used in the corrosive etching environment.

Effect of temperature.—The etchant temperature, like the concentration of HF species, can affect the kinetic resistance. It can also affect the mass-transfer resistance. Typically the kinetic rate increases with an increase in temperature because of the exponential dependence of the kinetic rate constant on the temperature. The mass-transfer rate also increases with temperature because both viscosity and density of liquids decrease with increasing temperature. Thus

$$\frac{\partial R_{r,HF}}{\partial T} < 0 \quad \text{and} \quad \frac{\partial k_{m,HF}}{\partial T} > 0 \text{ implies } \frac{\partial R_{m,eff,HF}}{\partial T} < 0 \quad [22]$$

Thus both $R_{r,HF}$ and $R_{m,eff,HF}$ decrease with increasing temperature. For reactions which have weak dependence on the temperature, kinetic effects increase with temperature, *i.e.,* $\partial(R_{m,eff,HF}/R_{r,HF})/\partial T < 0$ and for reactions which have strong dependence on the temperature, mass-transfer effects increase with increasing temperature, *i.e.,* $\partial(R_{m,eff,HF}/R_{r,HF})/\partial T > 0$. As shown in Fig. 18, when changes in both the kinetic and mass-transfer resistances are comparable, there is no incremental effect of temperature on the polishing efficiency, *i.e.,* $\partial(R_{m,eff,HF}/R_{r,HF})/\partial T \approx 0$. However, dependence of these parameters on the temperature can be different under different etching conditions. A few experiments conducted to study effects of temperature yielded unclear results.

Conclusions

Silicon etching is a mass-transfer influenced three-phase system. The three-phase etching system can be phenomenologically modeled as a two-phase system. Mass-transfer and kinetic influences on etching process are explained by the ratio of the effective mass-transfer resistance to the kinetic resistance.

A rough silicon wafer is a field of peaks and valleys characterized by an average roughness, ϕ. In a mass-transfer influenced system, etching rates at peaks are higher than the etching rates at valleys as a result of the difference in the local mass-transfer resistances. Thus, in the presence of the mass-transfer resistance chemical polishing takes place. Dependence of polishing efficiency (the ratio of actual polishing rate to the maximum possible polishing rate) on the ratio of effective mass-transfer resistance to kinetic resistance is explained using the proposed phenomenological model and experimental data.

Gaseous products of the etching reaction form the intrinsic bubbles that mask local sites on the silicon wafer surface, which leads to surface irregularities that are explained by the bubble-masking effect. The effects of the bubble detachment from the surface, and bubble and HF transport through the mass-transfer film are lumped in an effective mass-transfer resistance. In the absence of excessive bubble-masking effect, the polishing efficiency increases with the ratio of the effective mass-transfer resistance to the kinetic resistance, reaches an optimum and then decreases. When this ratio is greater than the critical bubble masking resistance value, the bubble-mask-

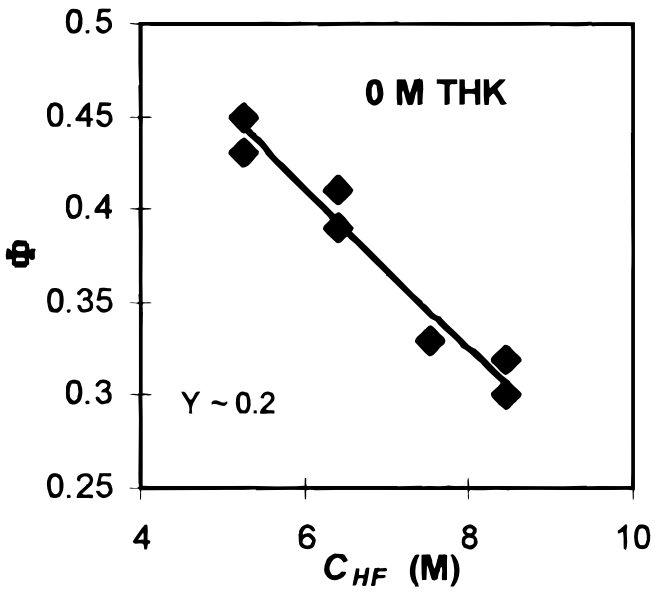

Figure 17. Effect of HF concentration on roughness.

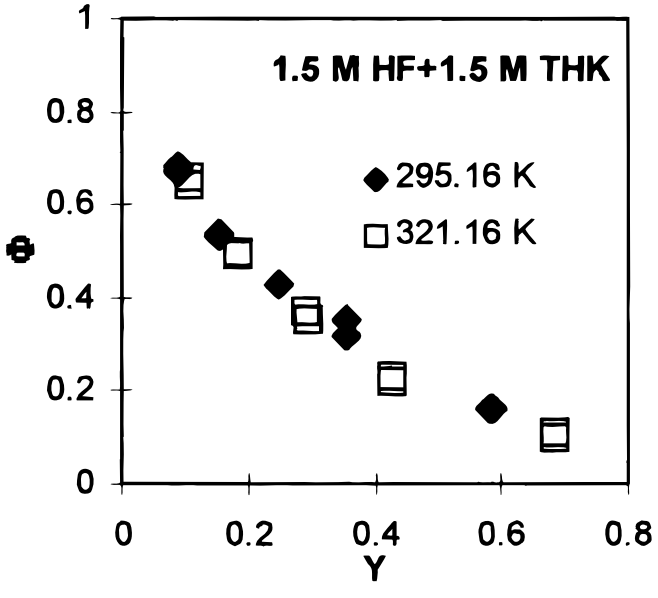

Figure 18. Effect of temperature on roughness.

S0013-4651(99)02-063-7 CCC: $7.00

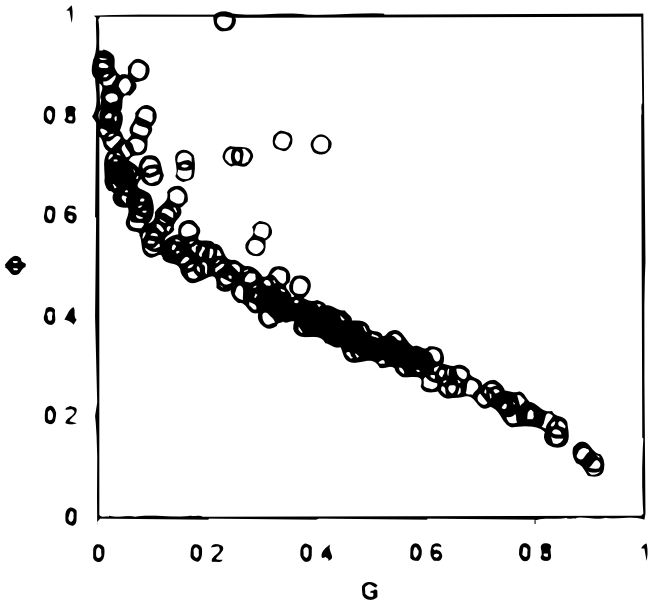

Figure A-1. A typical relationship between roughness and gloss.

ing is significant, and hence, the polishing efficiency decreases. Reduction in the polishing efficiency can also result by a reduction in the difference between the etching rates at peaks and valleys for very high mass-transfer resistances.

Addition of a thickener increases the mass-transfer resistance. Thus, the ratio of the mass-transfer resistance to kinetic resistance can be increased by addition of an inert thickener. Also, the kinetic resistance changes with changing HF concentration with negligible effect on the mass-transfer resistance. Hence, this ratio can also be controlled by varying the HF concentration. When both the mass-transfer resistance and kinetic resistance show comparable change with temperature, polishing efficiency does not change appreciably with temperature.

Thus, the ratio of the effective mass-transfer resistance to kinetic resistance must be higher than the critical minimum value and lower than the critical bubble masking value to achieve a high polishing efficiency.

Acknowledgments

The authors acknowledge the Operations Technology Department of MEMC at Kuala Lumpur for implementing the new etching process based on this research. The authors also thank Judy Schmidt, Shawn Patton, and Tom Doane for their help in conducting experiments.

MEMC Electronic Materials, Incorporated, assisted in meeting the publication costs of this article.

Appendix

In semiconductor industries "gloss" is used with "roughness" as a measure of polishing efficiency. Analysis on roughness can be translated to analysis on gloss. Gloss and roughness are quite closely related. Gloss is a measure of reflectance. Reflectance increases with decreasing or improving roughness. Figure A-1 shows a typical gloss to roughness relationship.

List of Symbols

C	concentration, mol/m^3
DF	driving force, mol/m^3
Ea	activation energy, J/mol
f	a function
G	dimensionless gloss
h	depth defined by local peak and valley on silicon surface, m
K	universal gas constant, J/mol K
k	mass-transfer coefficient or reaction rate constant, m/s
L	total length for roughness measurement, m
MT	mass transfer
R	resistance, s/m
RN	reaction
r	rate of a mechanism or process, mol/m^2 s
rl	rate of linear removal, m/s
SC	surface character
T	temperature, K
THK	thickener (phosphoric acid)
t	time, s
x	abscissa, m
Y	dimensionless removal
y	ordinate, m

Greek

Δ	total difference operator
δ	local film thickness, m
Φ	dimensionless roughness
ϕ	roughness, m
η	efficiency
λ	local roughness, m
μ	viscosity, kg/cm s
τ	characteristic time, s
ξ	conversion factor, m^3/mol of HF

Subscripts and superscripts

avg	average
b	liquid bulk conditions
bm	critical bubble masking value
eff	effective
f	interfacial (film)
g	gas phase, bubbles
HF	HF
HNO_3	HNO_3
i	a given species
inst	instantaneous
j	a given species
m	mass-transfer
max	maximum
min	minimum
o	overall
p	peaks
pol	polishing
r	reaction
s-l	surface to linear
sc	corresponding to surface character
T	temperature
thk	thickener
v	valleys
δ	local film thickness
μ	viscosity
1	initial condition
2	final condition

NB: multiple subscripts are separated by comma.

References

1. F. Shimura, *Semiconductor Silicon Crystal Technology,* pp. 184-186, Academic Press, Inc., San Diego (1989).
2. N. Moldovan and M. Ilie, *Mater. Sci. Eng.,* **B37,** 146-149 (1996).
3. H. Camon, Z. Moktadir, and M. Djafari-Rouhani, *Mater. Sci. Eng.,* **B37,** 142-145 (1996).
4. L. D. Dyer, G. J. Grant, C. M. Tipton, and A. E. Stephens, *J. Electrochem. Soc.,* **136,** 3016 (1989).
5. S. Verhaverbeke, I. Teerlinck, C. Vinckier, G. Stevens, R. Cartuyvels, and M. M. Heyns, *J. Electrochem. Soc.,* **141,** 2852 (1994).
6. H. Kikuyama, M. Waki, M. Miyashita, T. Yabune, and N. Miki, *J. Electrochem. Soc.,* **141,** 366 (1994).
7. D. J. Monk and D. S. Soane, *J. Electrochem. Soc.,* **140,** 2339 (1993).
8. B. Schwartz and H. Robbins, *J. Electrochem. Soc.,* **108,** 365 (1961).
9. A. F. Bogenschütz, W. Krusemark, K. H. Locherer, and W. Mussinger, *J. Electrochem. Soc.,* **114,** 970 (1967).
10. H. Robbins and B. Schwartz, *J. Electrochem. Soc.,* **106,** 505 (1958).
11. H. Robbins and B. Schwartz, *J. Electrochem. Soc.,* **107,** 108 (1960).
12. B. Schwartz and H. Robbins, *J. Electrochem. Soc.,* **123,** 1903 (1976).
13. D. L. Klein and D. J. D'Stefan, *J. Electrochem. Soc.,* **108,** 37 (1962).
14. H. Erk and R. Vandamme, U.S. Pat. 5,340,437 (1994).
15. D. G. Schimmel, *J. Electrochem. Soc.*, **123,** 734 (1976).
16. D. R. Turner, *J. Electrochem. Soc.,* **108,** 561 (1961).
17. K. S. Nahm, Y. H. Seo, and H. J. Lee, *J. Appl. Phys.,* **81,** 2418-2424 (1997).

S0013-4651(99)02-063-7 CCC: $7.00

18. D. G. Schimmel and M. J. Elkind, *J. Electrochem. Soc.,* **125,** 152 (1978).
19. R. W. Fathauer, T. George, A. Ksendzov, and R. P. Vasquez, *Appl. Phys. Lett.,* **60,** 995 (1992).
20. K. Gaffney and H. D. Chiou, Abstract 502, The Electrochemical Society Meeting Abstracts, Vol. 98-1, San Diego, CA, May 3-8, 1998.
21. Th. Bauer, L. Farbry, T. Teuschler, G. Schwab, and M. Stadler, Abstract 321, The Electrochemical Society Meeting Abstracts, Vol. 98-1, San Diego, CA, May 3-8, 1998.
22. I. E. Berishev, F. De Anda, V. A. Mishournyi, J. Olvera, N. D. Ilyinskaya, and V. I. Vasilyev, *J. Electrochem. Soc.,* **142,** L189 (1995).
23. K. McAndrews and P. Sukanek, *J. Electrochem. Soc.,* **138,** 863 (1991).
24. J. P. John and J. McDonald, *J. Electrochem. Soc.,* **140,** 2622 (1993).
25. K. Osseo-Asare, D.Wei, and K. K. Mishra, *J. Electrochem. Soc.,* **143,** 749 (1996).
26. D. J. Monk, D. S. Soane, and R. T. Howe, *J. Electrochem. Soc.,* **141,** 264 (1994).
27. D. J. Monk, D. S. Soane, and R. T. Howe, *J. Electrochem. Soc.,* **141,** 270 (1994).
28. D. J. Monk, D. S. Soane, and R. T. Howe, *Thin Solid Films,* **232,** 1 (1993).
29. Y. Kunii, S. Nakayama, and M. Maeda, *J. Electrochem. Soc.,* **142,** 3510 (1995).
30. T. Aoyama, T. Yamazaki, and T. Ito, *J. Electrochem. Soc.,* **143,** 2280 (1996).
31. O. Levenspiel, *Chemical Reaction Engineering,* 2nd ed., p. 349, Wiley Eastern Limited, New Delhi (1972).
32. R. H. Perry and D. W. Green, *Chemical Engineer's Handbook,* 6th ed., pp. 4.1-4.91, McGraw-Hill, Inc., New York (1984).
33. E. L. Cussler, *Diffusion-Mass Transfer in Fluid Systems,* pp. 75-78, Cambridge University Press, Cambridge (1984).